energies

MDPI

Article

Performance Analysis of a 300 MW Coal-Fired Power Unit during the Transient Processes for Peak Shaving

Chunlai Yang [1,*,†], Xiaoguang Hao [1], Qijun Zhang [2,†], Heng Chen [2], Zhe Yin [1] and Fei Jin [1]

[1] State Grid Hebei Energy Technology Service Co., Ltd., Shijiazhuang 210023, China
[2] School of Energy Power and Mechanical Engineering, North China Electric Power University, Beijing 102206, China; heng@ncepu.edu.cn (H.C.)
* Correspondence: yangchunlai1987@126.com
† These authors contributed equally to this work.

Abstract: A simulation model based on Dymola modelling was developed to investigate the dynamic characteristics of automatic generation control (AGC) for variable-load thermal power units in this study. Specifically, a 300 MW unit from a power plant in northern China was used to verify the model's validity in steady-state processes and to analyze the behavior of the main thermal parameters under different rates of load changes. The economic performance of the unit under different rates of load changes is also analyzed by combining the economic indexes of "two regulations" in the power grid. Results indicate that as the rate of load changes increases, boiler output, main steam temperature, reheat steam temperature, main steam pressure, and working temperatures of various equipment fluctuate more intensely. Specifically, at a rate of load reduction of 2.0% P_e MW/min, the maximum deviation of the main steam temperature can reach 7.6 °C, with the screen-type superheater experiencing the largest heat exchange. To achieve a balance between safety and economics for the unit, the rate of load raising should not exceed 1.2% P_e MW/min, and the rate of load reduction should not exceed 0.8% P_e MW/min. This paper applies the covariance index and AGC assessment index of the thermal power unit load control system to the established dynamic simulation model to supplement the AGC assessment index in the "two regulations", and to provide a flexible and reasonable system evaluation result for field operators to refer to, so as to improve the economics of the system on the basis of safety.

Keywords: coal-fired power plant; power regulation; transient simulation; dynamic characteristics; performance optimization

Citation: Yang, C.; Hao, X.; Zhang, Q.; Chen, H.; Yin, Z.; Jin, F. Performance Analysis of a 300 MW Coal-Fired Power Unit during the Transient Processes for Peak Shaving. *Energies* **2023**, *16*, 3727. https://doi.org/10.3390/en16093727

Academic Editor: Dimitrios Katsaprakakis

Received: 21 March 2023
Revised: 17 April 2023
Accepted: 24 April 2023
Published: 26 April 2023

1. Introduction

With the rapid development of society and economics, a significant amount of fossil fuels, including coal and petroleum, have been consumed, leading to severe pollution and greenhouse gas emissions [1]. In response, numerous governments have become motivated to develop ambitious plans for energy production from renewable sources [2]. Renewable energy sources, such as solar, wind, and hydro energy, offer a clean and abundant alternative to fossil fuels with zero greenhouse gas emissions [3]. However, the stochastic nature and variability of wind and solar power sources pose considerable obstacles to power grid management [4]. The increasing demand for peak-load shaving requires abundant dispatchable power plants for power regulation [5]. Therefore, conventional power sources must perform with greater flexibility to effectively utilize renewable energy [6]. Addressing the load fluctuations in high renewable energy penetration power systems with quick responses has become a focal point of research in recent years [7].

Some papers have investigated the economics of power systems in other developing countries with high penetration of renewable energy sources such as wind, solar, and hydro. Acaroğlu et al. [8] used an autoregressive distributed lag (ARDL) time series approach

to analyze the relationship between environmental degradation, economic growth, trade openness, primary energy consumption, coal consumption, and hydropower consumption in Turkey from 1971 to 2015. The results of the study emphasize the importance of renewable energy use in reducing environmental degradation and coal use in increasing environmental degradation. Harrucksteiner et al. [9] assessed the economic potential of solar and wind energy in Mongolia based on physical geographic constraints (e.g., slope) and socio-geographic constraints (e.g., protected areas). Bhanja et al. [10] developed an electricity supply system sustainability index for each city in India to measure each city based on its sustainable power generation and distribution system. Finally, the TOPSIS methodology was used to identify the solar cities with the highest technical and economic potential to successfully achieve the goals of the Solar Cities Mission. Wang et al. [11] examined the role of nuclear, hydro, and biomass energy on China's overall ecological footprint, incorporating quarterly data from 1970Q1 to 2020Q4, and used quantitative causality based on means and variances for an empirical analysis, which suggests that clean energy should be deployed rapidly and widely before the ecological footprint peaks. Otherwise, the role of nuclear, biomass, and hydro energy in reducing emissions may decline. Timilsina et al. [12] analyzed the economics of stylized grid-connected distributed PV implemented in the residential, commercial, and industrial sectors in Bangladesh and developed an economic model for the analysis. Therefore, the economics of high penetration of renewable energy sources such as wind, solar, and water are highly valued in all developing countries. Coal-fired power plants are currently predominant in China's power system, with coal-fired generating units serving as the primary force for power regulation [13]. Although China has been increasing its installed capacity of peaking power resources, such as pumped-hydro energy storage and gas-fired power, they are still inadequate to meet the demand for peak shaving. As a result, coal-fired power units will continue to play the primary role in load regulation in the foreseeable future [14]. Coal-fired units continue to serve as the primary peak-shaving service providers from a national perspective [15]. Power plant operators have implemented several measures to respond to the load-regulating requirements of power grids, including the reduction of low-load operation and continuous operation at an off-design point [16]. However, due to the nonlinearity of the boiler-turbine system, rapid changes in the generating load of a coal-fired power unit, such as during loading, de-loading, or ramping, may result in fluctuations in steam temperature, causing negative impacts on other parameters and reducing overall flexibility and thermal performance [17]. Therefore, it is crucial to enhance the ability to adjust load variation in a swift, safe, and high-efficiency manner for coal-fired power plants, especially given the high penetration of renewable energy in power systems.

Modifying the thermal system configurations of coal power units can improve their operational flexibility [18]. Much research has been conducted on the system optimization and performance evaluation of coal power plants for promoting load regulation [19–21]. Besides, the transient characteristics and related control strategies of power generation units during load variations have drawn a critical mass of attention. For example, Hentschel et al. [22] investigated the detailed modelling of a coal-fired power plant using the thermohydraulic simulation code Apros and accomplished dynamic systematic simulation with very small error values as compared to process data. Wang et al. [23] investigated the dynamic performance of thermal power plants during load cycling processes, taking into account the interaction between thermal systems and control systems. Feasible strategies were developed for optimizing the coordinated control systems to improve peak shaving capabilities. Zhao et al. [24] used the GSE software to establish a transient simulation model of a 660 MW supercritical coal-fired power system. The model was used to examine six regulation measures aimed at rapidly activating the thermal storage in the thermal systems. Wang et al. [25] developed a novel method for controlling the steam temperatures in a double-reheat coal-fired power plant. The proposed approach was validated through dynamic modelling and applied to an operational double-reheat coal-fired power plant. Ma et al. [26] developed a dynamic model for a subcritical coal-fired power plant, utilizing

PID-based regulatory controllers. The main objective of the study was to maintain a stable main steam temperature at the boiler exit while also maximizing plant efficiency during ramping. To achieve this goal, an optimization approach was implemented. Yan et al. [27] utilized dynamic and exergy analysis models to evaluate the performance of a solar-aided coal-fired power plant during transient processes, taking into account solar irradiance disturbances and system regulation. Dai et al. [28] proposed a data mining-based multi-objective economic load dispatch method for coal-fired power plants. The method enables the mining of optimal decision-making samples from the offline database to guide on-line economic load dispatching based on the power grid's load demand. Ma et al. [29] constructed an integrated dynamic model of a supercritical CO_2 cycle and explored a synergistic control strategy for variable dynamic working conditions. Despite the substantial amount of research on the dynamic characteristics and flexibility improvement of coal-fired power plants, there remains a scarcity of literature on the evaluation of transient performance and the identification of suitable load change rates for coal power units.

The "two regulations" refer to two dispatching rules in the Chinese power system, namely the "Regulations on Automatic Dispatching of Power Systems" and the "Measures for the Operation and Management of Power Dispatching and Control Centers." The introduction of these two regulations not only provides robust institutional guarantees but also technical support to ensure the safe and stable operation of China's power system. This is highly significant for achieving efficient dispatching and management of the power system, promoting the growth of clean energy, and ensuring the security and reliability of the power supply.

However, in the available literature, there is hardly a standardised metric or precise definition to assess the dynamic performance of thermal power units in coal-fired power plants due to the influence of several factors such as the rate of load change, the combustion control strategy, the boiler water circulation system, and the turbine regulation system. In addition, different dynamic performance indicators may conflict with each other, such as the balance between economics and safety. It is the absence of this criterion that leads to a greater reliance on and constraint by operator experience in the actual operation of coal combustion, which poses a certain risk to safety. It is therefore a challenging and practical task to establish a comprehensive dynamic performance evaluation index system that takes into account multiple factors and is applicable to coal-fired power plants.

In order to tackle this issue, the present study constructed a dynamic model of a coal-fired power plant through the utilization of Dymola software, and its precision was validated. The advantages of dynamic modelling over steady-state modelling are obvious. Steady-state modelling can only simulate the results of a few design conditions; however, for actual operating units, the operating time under off-design conditions is quite long, which requires dynamic modelling to simulate the off-design conditions. Dynamic modelling can also study the control logic and the dynamic characteristics of the main parameters of the unit. However, dymola-based dynamic modelling has certain drawbacks, such as the need for extensive simplification of the control logic of the actual unit and the fact that the modelling needs to be carried out according to the design parameters, which need to be re-modelled for different units, making the application less generalisable. The research mainly focused on investigating the dynamic characteristics of the main heating surfaces in the boiler section and the main thermodynamic parameters of the turbine section when subjected to different load change rates controlled by load raising and reduction commands. The economic indicators and covariance indicators in the "two regulations" are quoted to fully assess the safety and economics of the device under different conditions. Based on the results, the maximum rate of load changes for the unit was determined, providing guidance for the actual operation of the unit. The comprehensive evaluation approach presented in this study is expected to contribute to the establishment of a standardized dynamic performance evaluation system for coal-fired power plants.

For a new coal-fired unit or one that has been in operation for a short period of time, the approach of using data modelling to evaluate the system is unrealistic due to the lack

of historical data to support it. Therefore, simulation software is needed to predict and evaluate the performance of the unit based on the design data. Through the evaluation indexes under different operating conditions, the system economics can be improved by increasing the variable load rate and reducing the internal heat storage of the unit as much as possible while ensuring safety. Therefore, combining this index with the simulation model will contribute to the improvement of coal-fired unit economics.

2. Reference Power Unit

For this study, a typical 300 MW subcritical coal-fired power plant was chosen as the subject of investigation. The plant is composed of a pulverized coal boiler, three turbines (including a high-pressure turbine, a medium-pressure turbine, and a low-pressure turbine), and an electric generator. Diagram of the reference coal-fired power unit is shown in Figure 1. Detailed information about the plant is presented in Table 1. Additionally, the steam cycle includes a thermal regeneration system with seven reheaters, and the parameters of the heat regeneration system are listed in Table 2.

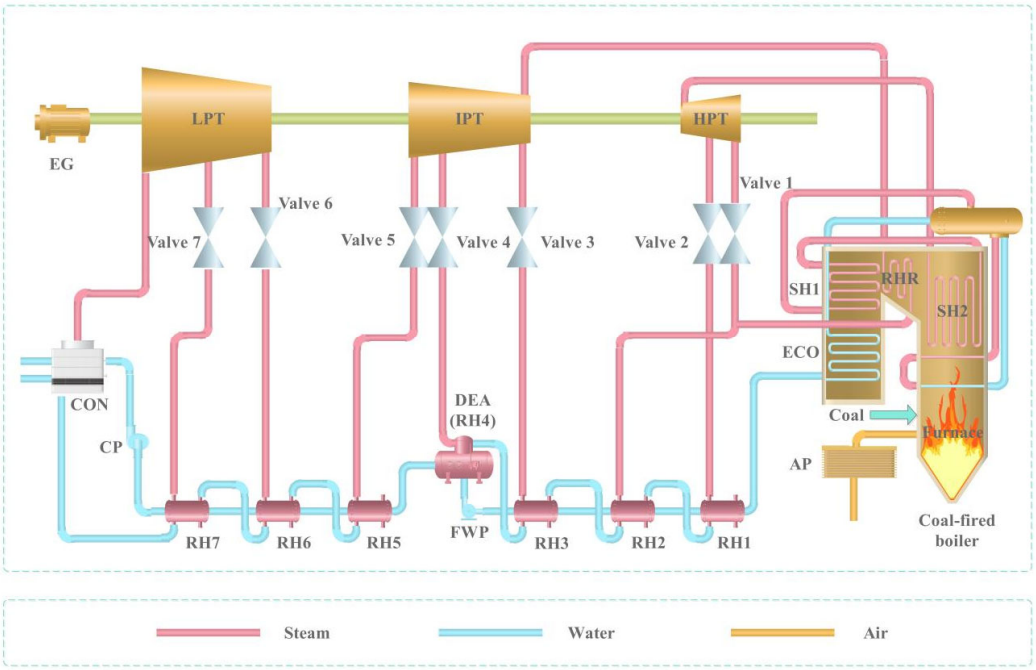

Figure 1. Diagram of the reference coal-fired power unit.

Table 1. Main parameters in the turbine side under 100% and 75% working conditions.

Parameters	Unit	Values	
		100% THA	75% THA
Power generation	MW	300.234	225.100
Main steam temperature	°C	538.0	538.0
Main steam pressure	MPa	16.670	13.250
Main steam flow rate	kg/s	260.38	189.80
Reheated steam temperature	°C	538.0	538.0
Reheated steam pressure	MPa	3.318	2.471
Reheated steam flow rate	kg/s	217.66	161.27
Cold reheat steam temperature	°C	325.3	302.0
Cold reheat steam pressure	MPa	3.687	2.745

Table 1. *Cont.*

Parameters	Unit	Values	
		100% THA	75% THA
Cold reheat steam flow rate	kg/s	217.66	161.27
Feedwater temperature	°C	272.2	253.1
Feedwater pressure	MPa	16.770	16.770
Feedwater flow rate	kg/s	260.38	189.80

Table 2. Design data of the heat regeneration system of the reference coal-fired power unit under 100%THA working conditions.

Item		RH1	RH2	RH3	DEA (RH4)	RH5	RH6	RH7
Extraction steam	Temperature (°C)	381.7	325.3	443.0	356.4	295.1	200.7	100.7
	Pressure (MPa)	5.5498	3.5763	1.7123	0.9066	0.5590	0.2287	0.0786
	Flow rate (kg/s)	17.08	20.01	8.44	7.48	11.01	10.51	11.64
Outlet feedwater	Temperature (°C)	270.5	243.8	204.7	175.7	156.1	124.5	93.0
	Pressure (MPa)	16.77	16.78	16.79	1.68	1.68	1.69	1.70
	Flow rate (kg/s)	260.38	260.38	260.38	260.38	206.28	206.28	206.28

3. Model Development and Validation

3.1. Model Development

To investigate the dynamic behavior of coal-fired power plants and enhance their operational flexibility, transient simulation is a viable approach under varying operating conditions [30]. The Dymola platform was utilized in this study to develop a transient model (Figure 2) of a representative 300 MW subcritical coal-fired power plant. Dymola is a powerful tool for modelling and simulating complex systems in engineering using the open Modelica modelling language, which describes system behavior through mathematical equations [31]. It supports hierarchical model composition, libraries of reusable components, and composite acausal connections. As shown in Figure 2, the structural properties of the system, including components, connectors, and connections, are created using a graphical editor, while equations and declarations are edited using a built-in text editor. The modelling details of the reference power unit are provided in Table 3.

The control system is crucial for the dynamic characteristics of coal-fired units, as coal, water, and wind are the primary inputs. Therefore, the control system for these inputs during load changes should be modeled with great care. The modelling details of the control system for the reference coal-fired unit in Dymola are presented in Table 4.

3.2. Basic Assumptions

Several simplifying assumptions were made in the modelling and analysis of the system, including the following assumptions:

1. Primary and secondary air were treated as equivalent, and the required volume of air for combustion was assumed to enter the furnace chamber after preheating through the air preheater;
2. Air and flue gas side air leakage and heat dissipation losses were ignored;
3. Run-off and leakage steam on the steam turbine side that did not perform work were not considered;
4. Air was assumed to consist of 21% oxygen by volume and 79% nitrogen at standard temperature and pressure conditions (25 °C and 1.01325 MPa).

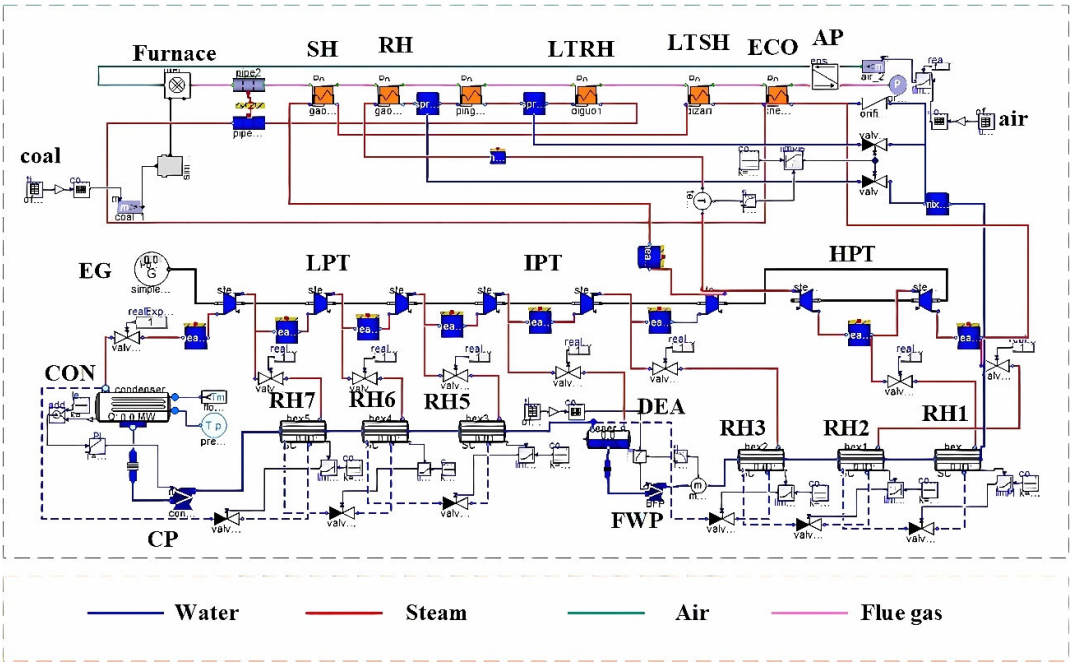

Figure 2. Transient simulation model of the reference coal-fired power unit in Dymola.

Table 3. Modelling details of the reference coal-fired power unit in Dymola.

Component	Details
Boilers	Constant heat transfer heat exchanger correlations; Infinite heat transfer/radiation between furnace gas volume and the riser tubes; Only radiation heat transfer to the riser tubes.
Turbines	Following Stodola's law (infinite number of stages); Constant isentropic efficiency; No energy or mass storage; No shaft inertia; The mechanical efficiencies are 99.80%.
RHs	The upper terminal temperature difference of RH1 is −0.7 °C, the upper terminal temperature difference of RH2, RH3, and RH4 is 0 °C, and the upper terminal temperature difference of the other RHs is 2.8 °C; The lower terminal temperature difference of RH4 is 0 °C, and the lower terminal temperature difference of the other RHs is 5.6 °C.
CONs	Thermodynamic equilibrium between liquid and vapor phases, i.e., no subcool; Heat transfer model uses the inflow steam quality to calculate the vapor phase; Reynolds number, no slip is assumed; No reduction of heat transfer area when the liquid level rises over the cooling tubes; No pressure loss on the cooling side.
Pumps	The isentropic efficiencies are 83.00%.
EG	The generator efficiencies is 98.95%.

Table 4. Modelling details of some essential control systems for reference coal-fired units in Dymola.

Component	Details
Airflow control system	Real-time monitoring of the coal amount in the furnace chamber is carried out, and the amount of air entering the furnace chamber is adjusted accordingly based on the current load command and the real-time coal volume control valve. This adjustment is made by setting the excess air coefficient for different load commands. The excess air coefficients are set to 1.2 for all 90–100% THA conditions, 1.3 for 75% THA conditions, and uniformly varying for 75% THA-90% THA conditions.
Feed coal control system	The coal feed quality corresponding to the different load orders is set. The real-time output power and load commands are monitored at any given moment, and the coal feed is increased or decreased using PID control. The feed coal mass flow rate is set at 69.72 kg/s for 100% THA operation and 55.78 kg/s for 75% THA operation, uniformly varying for 75% THA-100% THA conditions.
Feed water control system	The feed water flow corresponding to the different load commands is set. The real-time feed water quantity and the design value of the feed water quantity corresponding to the load command are monitored at a given moment, and the feed water quantity is increased or decreased by controlling the speed of the feed water pump using PID control. The feed water mass flow rate is set at 260.38 kg/s for 100% THA operation and 189.80 kg/s for 75% THA operation, uniformly varying for 75% THA-100% THA conditions

3.3. Model Validation

A comparison of the key unit parameters between 100% THA and 75% THA operating conditions is presented in Table 5. The majority of the main parameters exhibit an error of 2% or less. However, some of the parameters related to reheated steam exhibit an error of up to 4%. This is primarily due to the omission of the steam turbine leakage component in the modelling process, resulting in an overestimation of the cold reheat steam flow rate and the reheat steam flow rate. Consequently, the reheat steam-related parameters exhibit a relatively large error. Overall, the error in the main parameters remains within 4% for both operating conditions, which satisfies the requirements of the project.

Table 5. Comparison of main unit parameters under 100% THA and 75% THA working conditions.

Parameters	Unit	Condition	Design Values	Simulation Values	Error
Power generation	MW	100% THA	300.230	300.243	0.00%
		75% THA	225.118	225.100	−0.01%
Main steam temperature	°C	100% THA	538.0	537.9	−0.02%
		75% THA	538.0	537.8	−0.04%
Main steam pressure	MPa	100% THA	16.670	16.698	0.36%
		75% THA	13.250	13.289	0.37%
Main steam flow rate	kg/s	100% THA	260.38	260.37	0.00%
		75% THA	189.80	190.00	0.11%

Table 5. *Cont.*

Parameters	Unit	Condition	Design Values	Simulation Values	Error
Reheated steam temperature	°C	100% THA	538.0	537.6	−0.07%
		75% THA	538.0	536.2	−0.33%
Reheated steam pressure	MPa	100% THA	3.318	3.390	2.17%
		75% THA	2.471	2.574	3.08%
Reheated steam flow rate	kg/s	100% THA	217.66	220.17	1.15%
		75% THA	161.27	166.83	3.45%
Feedwater temperature	°C	100% THA	272.2	275.2	1.10%
		75% THA	253.1	259.4	2.49%
Feedwater pressure	MPa	100% THA	16.770	16.808	0.23%
		75% THA	13.350	13.347	−0.02%

4. Results and Discussion

4.1. Dynamic Performance of the Steam Turbine

The coal-fired units were subjected to steady operation at 100% THA for 0–10,000 s, followed by load reduction at rates of 0.5%, 1%, 1.5%, and 2% P_e/min to reach 75% THA by 10,000 s. The units then operated steadily at 75% THA until 15,000 s during the load reduction process. Conversely, during the load raising process, the units were operated steadily at 75% THA for 0–10,000 s and then subjected to load raising at rates of 0.5%, 1%, 1.5%, and 2% P_e/min to reach 100% THA by 10,000 s. The units then operated steadily at 100% THA until 15,000 s during the load raising process. To facilitate further analysis, the time range of 9500–15,000 s was selected for further study.

The dynamic characteristics of the output power are shown in Figure 3, where the greater the rate of load changes, the greater the variation in output power. Notably, load raising exhibits slightly lower variations in output power compared to load reduction. The largest overshoot occurs during load reduction at a rate of 2.0% P_e MW/min, with a magnitude of approximately 1.8 MW.

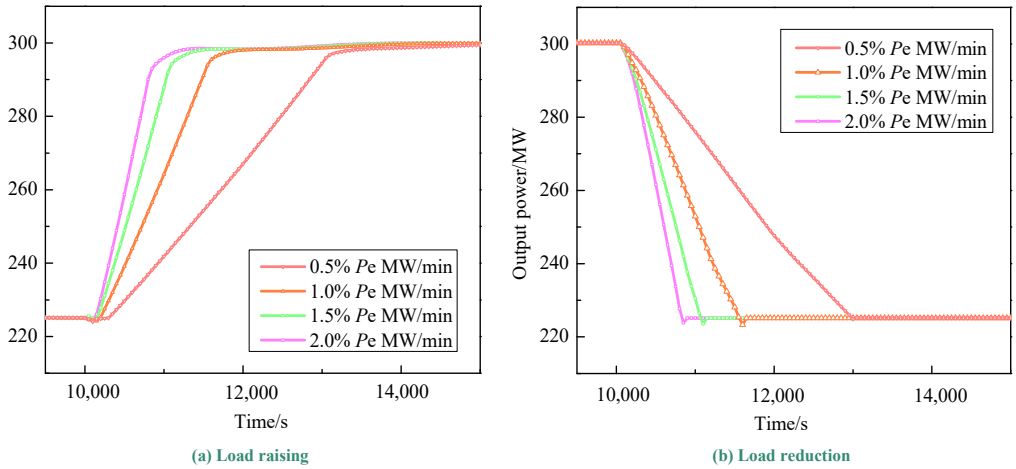

Figure 3. Dynamic performance of output power during load change processes.

The dynamic characteristics of the main steam temperature are shown in Figure 4, which demonstrates that the main steam temperature undergoes significant changes in response to load variations. Specifically, as the rate of load change increases, so does the magnitude of the corresponding changes in the main steam temperature. During load reduction, the main steam temperature exhibits an initial rise followed by a return to 538 °C,

whereas during load increase, the opposite is observed. Furthermore, the changes in the main steam temperature during load raising are considerably smaller than those during load reduction.

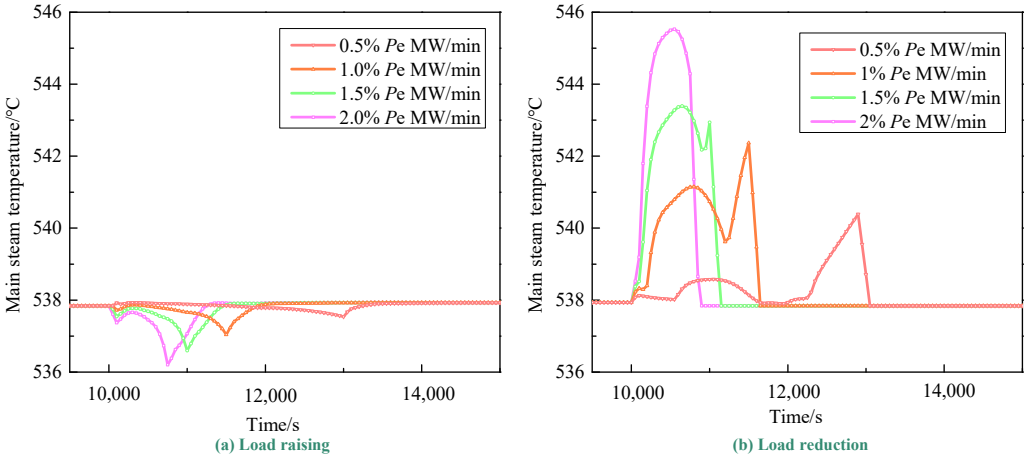

Figure 4. Dynamic performance of the main steam temperature during load change processes.

At a load reduction rate of 2.0% P_e MW/min, the maximum deviation in the main steam temperature is 7.6 °C, which is lower than the commonly acceptable limit of 8 °C deviation for actual operation. However, if the rate of load change is further increased or the peak shaving demand reaches a lower level, the impact of the main steam temperature should be taken into account.

The dynamic characteristics of the reheated steam temperature are depicted in Figure 5, indicating that the reheated steam temperature undergoes significant changes in response to load variations. Specifically, as the rate of load change increases, so does the magnitude of the corresponding changes in the reheated steam temperature. During load reduction, the reheated steam temperature exhibits an initial rise followed by a return to 538 °C, while the opposite is observed during load increase. Furthermore, the changes in the reheated steam temperature during load raising are slightly smaller than those during load reduction.

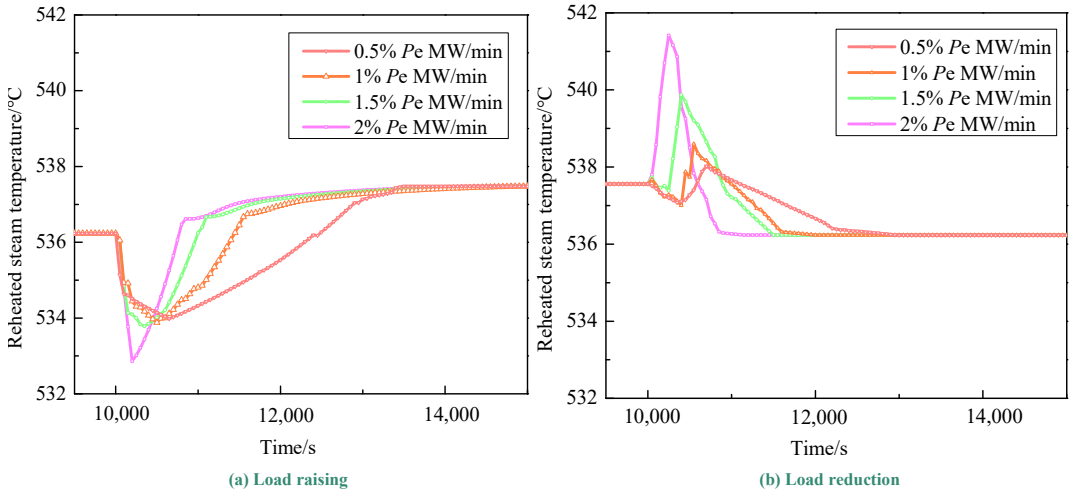

Figure 5. Dynamic performance of reheated steam temperature during load change processes.

At a load reduction rate of 2.0% P_e MW/min, the maximum deviation in the main steam temperature can reach 3.9 °C. It should be noted that, although the design value for the reheat steam temperature is 538 °C for both 100% THA and 75% THA operation, the simulated value for the reheat steam temperature during 75% THA operation can no longer

reach 538 °C but only rises to 536.2 °C. Therefore, when the load needs to be reduced to a lower level, the dynamic characteristics of the reheated steam temperature should be fully considered to avoid the negative impact of a lower reheat steam temperature on the cycle thermal efficiency.

The dynamic characteristics of main steam pressure are shown in Figure 6, revealing that the magnitude of the corresponding changes in output power increases with the rate of load changes. Notably, the variation in output power during load raising is slightly smaller than that during load reduction. Furthermore, the observed overshoot is relatively small. The relationship between main steam pressure and output power is also mentioned later in the study.

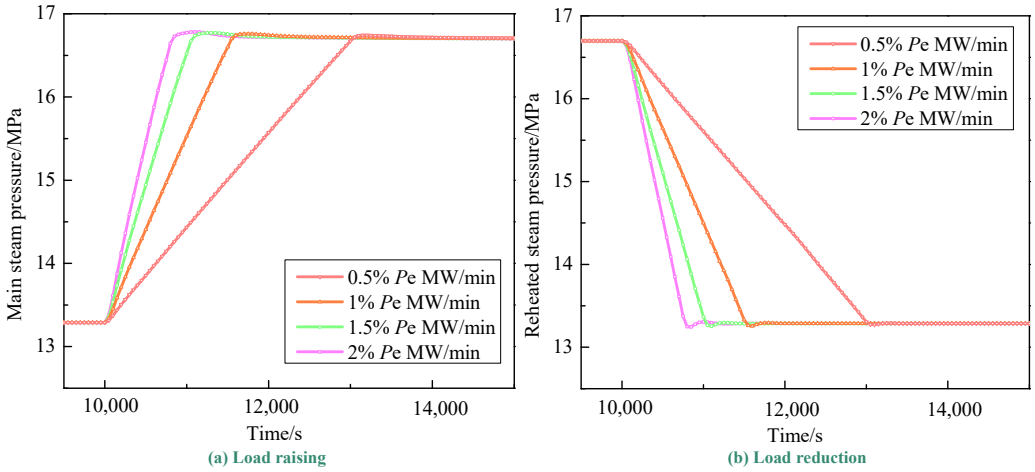

Figure 6. Dynamic performance of main steam pressure during load change processes.

4.2. Dynamic Performance of the Boiler

During the load change processes, the working mass temperature of the heating surface in each piece of equipment in the boiler undergoes more drastic changes compared to the turbine temperature. To investigate this phenomenon, three representative areas and exhaust gases are selected, and the dynamic characteristics of the working mass temperature of each piece of equipment in the boiler are analyzed and compared.

Figures 7 and 8 illustrate the dynamic change curves of the working mass temperature on different heating surfaces of the boiler during varying load change rates. The results indicate that the outlet temperature of the coal economizer and exhaust gases increases with load, while the outlet temperature of the low-temperature reheater and low-temperature superheater decreases with load. Additionally, the rate of load changes is directly proportional to the extent of temperature changes across different heating surfaces in the boiler. The coal economizer and low-temperature reheater outlet temperatures show negligible fluctuations, whereas the outlet temperatures of the low-temperature superheater and exhaust gases experience significant variations.

It should be noted that the typical design value for the outlet temperature of exhaust gases is approximately 110–160 °C. However, under 75% THA working conditions, the simulated value for the outlet temperature of exhaust gases reaches 113 °C. If the outlet temperature of exhaust gases is too low, it may cause low-temperature corrosion on the tail heating surface. Furthermore, a low outlet temperature of exhaust gases can reduce the heat transfer temperature difference of the tail heating surface, requiring more heating area and increasing metal consumption, boiler ventilation resistance, and fan power consumption. Therefore, when the load command is set to a lower level, the limits of the outlet temperature of exhaust gases at the peaking depth should be taken into full consideration.

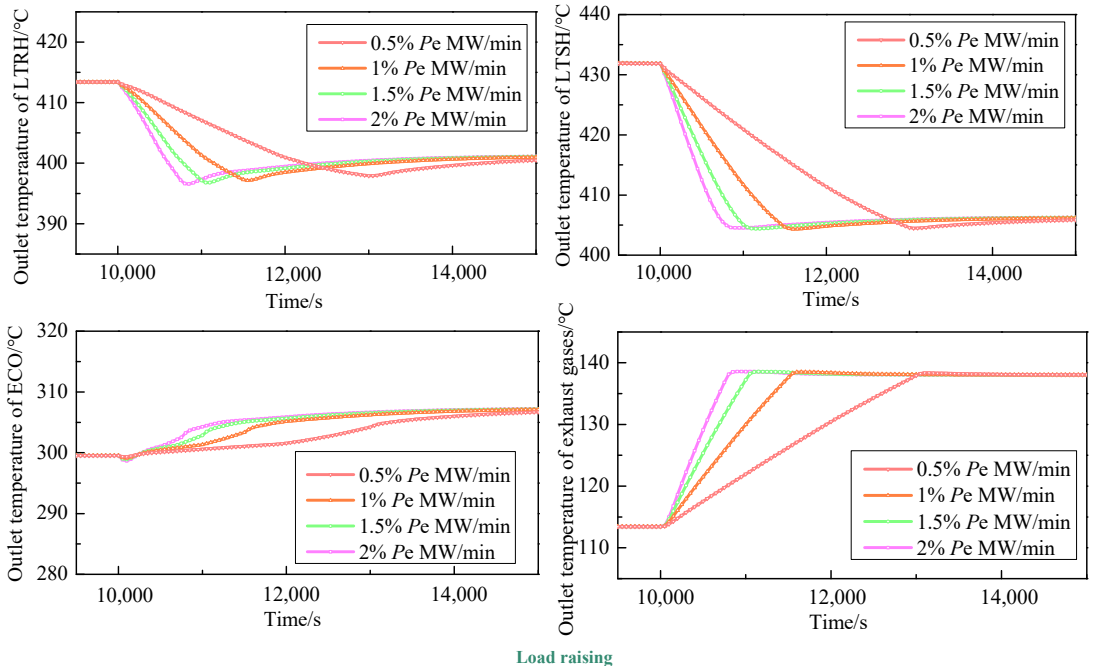

Figure 7. Dynamic performance of different boiler heating surface temperatures during load raising.

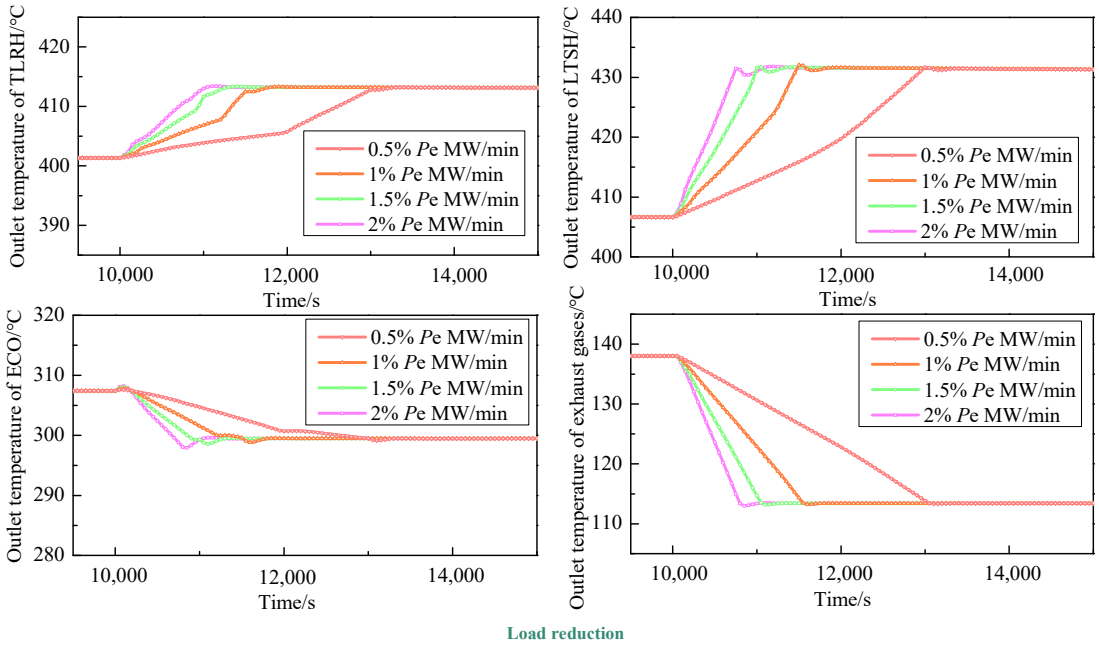

Figure 8. Dynamic performance of different boiler heating surface temperatures during load reduction.

According to Figure 9, it can be observed that the heat exchange of each heat transfer surface at 75% THA operating conditions is less than 75% of the heat exchange at 100% THA operating conditions. The screen-type superheater has the maximum heat exchange, reaching a value of 85.8 MW at 100% THA operating conditions.

Excessive heat exchange in the boiler may cause significant changes in the water level, which can affect the water circulation and steam-water separation in the boiler. The observed variations in the outlet temperature of the low-temperature superheater and exhaust gases, while the outlet temperature of the coal economizer and low-temperature reheater exhibit minimal variations, may have an adverse effect on the thermal efficiency of the boiler. This can subsequently impact the operational costs and benefits of the entire

thermal power plant. Thus, it is essential to pay more attention to the heat exchange of the screen-type superheater to prevent such faults during load instruction changes.

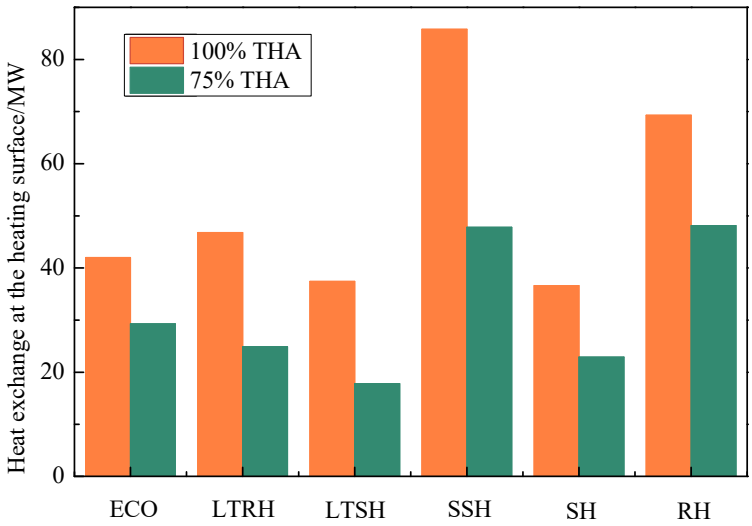

Figure 9. Heat exchange at steady state for each heating surface.

4.3. Performance Evaluation of Power Unit

The "two regulations" refer to a set of performance assessment criteria used to evaluate the performance of a power generation unit in three key areas: response time, regulation rate, and regulation accuracy. In order to calculate the economic index of the unit, it is important to identify the regulation rate index and the regulation accuracy index. These indices play a crucial role in determining the appropriate calculation method for the economic index.

The following equation defines the economics of the "two regulations" [27,32]:

$$I_{\mathrm{k}} = \lambda_{11} K_{\mathrm{V}} + \lambda_{22} K_{\mathrm{N}} \tag{1}$$

where K_{V} is the average regulation rate indicator of the unit; K_{N} is the regulation accuracy indicator; and λ_{11} and λ_{22} are the weighting coefficients, which are both taken as 0.5 in this paper.

The average regulation rate indicator is determined by the following equation:

$$K_{\mathrm{V}} = 1 - \frac{V_{\mathrm{m}}}{V_{\mathrm{b}}} \tag{2}$$

where V_{m} is the measured AGC regulation rate of the unit and V_{b} is the basic response rate of the unit.

$$V_{\mathrm{m}} = \alpha \cdot \frac{\Delta N}{T} \tag{3}$$

where α is the unit conversion factor; ΔN is the amount of change in the AGC load test command; and T is the time for the actual load of the unit to reach within the dead zone of the target value of the AGC test load command.

If the K_{V} value is less than 0, it means that the average regulation rate indicator is excellent, and in the subsequent calculations, the K_{V} value is treated as equal to 0.

The regulation accuracy indicator is determined by the following equation:

$$K_{\mathrm{N}} = \beta \cdot \frac{\int_0^T |N_{\mathrm{e}}(t) - N_0(t)| dt}{T} \tag{4}$$

where β is the accuracy deflation factor; $N_{\mathrm{e}}(t)$ is the actual output of the unit after AGC action; $N_0(t)$ is the target output of the unit after AGC action; and T is the AGC input time.

Joe et al. [33] proposed a performance evaluation index based on the determinant of the covariance matrix of the system output signal, which was formulated as an evaluation function. The benchmark data of the system's operation were used as a reference to calculate the covariance matrix determinant. The definition of the covariance evaluation metric I_V is as follows [34,35]:

$$I_V = \frac{|f_{cov}(y_M)|}{|f_{cov}(y_B)|} \tag{5}$$

where $f_{cov}(y_M)$ and $f_{cov}(y_B)$ each represent the determinant of the covariance matrix for the baseline period data B and the monitoring period data M.

The main steam pressure P_f and the real power N_e are two-dimensional variables, and the constructed covariance matrix is a two-dimensional matrix. As shown in the following formula:

$$f_{cov}(P_f, N_e) = \begin{bmatrix} D(P_f) & \mathrm{cov}(P_f, N_e) \\ \mathrm{cov}(N_e, P_f) & D(N_e) \end{bmatrix} \tag{6}$$

From the above equation, it can be seen that the choice of the reference period has a large impact on the evaluation index. Therefore a load reduction condition at a rate of 1.5% P_e MW/min was chosen as the baseline period. The above equations were calculated using MATLAB.

The "two regulations" AGC economic indicator in Equation (1) and the covariance indicator in Equation (5) define the comprehensive evaluation indicator I for thermal power units as follows:

$$I = \lambda_1 I_V + \lambda_2 I_k \tag{7}$$

where λ_1 and λ_2 are weighting factors, both greater than 0 and summing to a value of 1.

The coefficients λ_1 and λ_2 are relevant to the operation of the generator set, where smaller coefficients indicate lower degrees of consideration given to the performance being evaluated. When the load control system's safety and stability are already good, more focus can be given to the economics of the system by reducing λ_1 and increasing λ_2. However, the basic requirements of the system must not be completely disregarded. On the other hand, if the safety and stability of the load control system are already difficult to ensure, it is not reasonable to focus on the economics of the system, and therefore λ_1 should be increased and λ_2 should be decreased, with the results of the integrated indexes reflecting mainly the basic indexes of the system. If there is a need to balance the evaluation of system safety and economics, the values of λ_1 and λ_2 should be as close as possible. Hence, the values of λ_1 and λ_2 are determined under three conditions:

(1) When the assessment prioritizes economics, take λ_1 as 0.41 and λ_2 as 0.59;
(2) When a balance between safety and economics is required, take λ_1 as 0.5 and λ_2 as 0.5;
(3) When the assessment prioritizes safety and stability, take λ_1 as 0.63 and λ_2 as 0.37.

The criteria for evaluating the overall performance of the AGC during the monitoring period are presented in Table 6.

Table 6. Criteria table for judging the overall performance of AGC during monitoring periods.

I	***I***	**Results of Assessment**
$0 < I < 0.37$	-	Excellent
$0.37 \leq I < 0.53$	-	Good
$0.53 \leq I < 1.47$	$0 \leq Iv < 1.1$	Medium
$0.53 \leq I < 1.47$	$Iv \geq 1.1$	Poor
$I \geq 1.47$	-	Poor

To investigate the maximum rate of load changes, additional simulation experiments were conducted at intervals of 0.1% P_e MW/min, ranging from 0.5% P_e MW/min to 2.0% P_e MW/min. The primary objective was to assess the variations in output power and main steam pressure and compute relevant performance indicators using the aforementioned formulas. The unit and control system's performance were initially evaluated in condition two, with λ_1 and λ_2 set to 0.5. The results of the evaluation for selected load change rates are presented in Table 7, and the assessment outcomes are illustrated in Figure 10.

Table 7. The specific assessment results for part of rate of the load changes under condition two.

The Rate of Load Changes		I_k	I_V	I	Results of Assessment
Load raising	0.5% P_e MW/min	0.55	0.13	0.34	Excellent
	1.0% P_e MW/min	0.46	0.44	0.45	Good
	1.5% P_e MW/min	0.34	0.92	0.63	Medium
	2.0% P_e MW/min	0.19	1.22	0.71	Poor
Load reduction	0.5% P_e MW/min	0.60	0.26	0.43	Good
	1.0% P_e MW/min	0.52	0.58	0.55	Medium
	1.5% P_e MW/min	0.38	1	0.69	Medium
	2.0% P_e MW/min	0.28	1.32	0.80	Poor

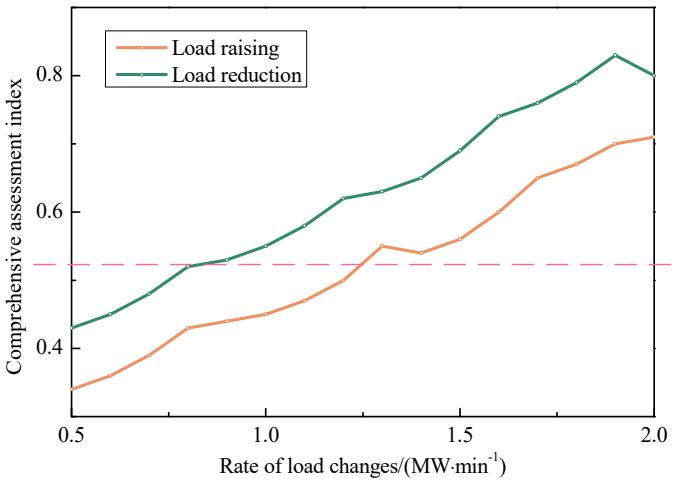

Figure 10. The result of assessment for different rates of load change.

The findings depicted in Figure 10 demonstrate that, as a general trend, the comprehensive assessment index increases with higher rates of load change, indicating poorer performance. Furthermore, the comprehensive evaluation indicators exhibit lower values during load raising as opposed to load reduction, implying that the load raising process is more economical and safer than the load reduction process at the same rate of load changes. This outcome can be attributed to the slower response time in the load reduction process and the greater fluctuations in the main parameters, leading to slightly higher covariance and economic indicators compared to the load raising process. It is deemed acceptable if the assessment result is rated as excellent or good, while a rating of medium or poor is considered substandard.

It is worth noting that the output power was taken every 5 s during the Dymola taking process, which led to a slight error in the calculation of Equation (4), as we had to approximate the integral formula.

The assessment result is considered to be met if the result is excellent or good, and it is considered substandard if the result is medium or poor. The results of the analysis for the above three conditions are shown below:

Under condition two, where a balance between safety and economics is required, it is preferable that the rate of load raising should not exceed 1.2% P_e MW/min and the rate of load reduction should not exceed 0.8% P_e MW/min.

However, if the simulated load control system has excellent process control performance characteristics and the combined indicators focus on the economics of the simulated load control system's participation in grid-connected auxiliary services, the rate of load raising should preferably not exceed 1.4% P_e MW/min and the rate of load reduction should not exceed 0.9% P_e MW/min under condition one.

When the load control system's safety performance is inadequate and significantly deviates from the load instructions, it becomes essential to guarantee the safety of system operation, unit operators, and the regular operation of the power system. In such cases, the comprehensive evaluation index focuses more on the safety of the load control system, with economic indicators carrying less weight. Thus, under condition three, it is recommended that the rate of load raising should not exceed 1.1% P_e MW/min and the rate of load reduction should not exceed 0.7% P_e MW/min to maintain the safety of the load control system's operation.

5. Conclusions

(1) A simulation model based on the Dymola platform was developed for a 300 MW unit and its major control system at a power plant in northern China, and its steady-state process was verified. The dynamic characteristics of the main thermal parameters of the unit are also studied under different load change rates according to the model. The results show that the larger the load change rate, the more obvious the changes in each main thermal parameter are.

(2) The simulation model was combined with the "two regulations" automatic generation control assessment index of the power system to determine the ultimate rate of load changes for the unit. This was conducted by considering the operating performance of the system and the economics of participating in automatic generation control regulation. The results showed that for this unit, under the condition of balancing economics and safety, the rate of load raising should not exceed 1.2% P_e MW/min and the rate of reduction should not exceed 0.8% P_e MW/min.

(3) The model construction method and the system evaluation index can be used to provide some guidance to field operators to maximize the variable load rate to improve economies while ensuring safety; however, there are still some shortcomings in the study, i.e., the model was constructed using the design data of the power plant, and if it is to be applied, the control logic and parameters in the model need to be readjusted. In the future, it is hoped that modelling can be carried out for 600 MW class units to facilitate the application of the research results. Based on the results of this study, it is recommended that the peaking and frequency regulation capabilities of thermal power units be given more importance and that uniform and clearer evaluation indicators be introduced to guide the operation of individual power plants.

Author Contributions: Conceptualization, C.Y.; methodology, C.Y.; software, H.C.; validation, H.C.; formal analysis, Z.Y.; investigation, Z.Y.; resources, F.J.; data curation, F.J.; writing—original draft preparation, Q.Z.; writing—review and editing, Q.Z.; visualization, X.H.; supervision, X.H.; project administration, X.H.; funding acquisition, X.H. All authors have read and agreed to the published version of the manuscript.

Funding: This work was funded by the Science and Technology Project of the State Grid Hebei Electric Power Co. (No. TSS2022-04).

Data Availability Statement: Due to restrictions (e.g., privacy or ethical), the data presented in this study are available on request from the corresponding author. The data are not publicly available as they will be used for writing subsequent papers and further analysis.

Acknowledgments: This work was supported by the Science and Technology Project of the State Grid Hebei Electric Power Co. (No. TSS2022-04).

Conflicts of Interest: The authors declare no conflict of interest.

Nomenclature

Symbols			
I	index		
Superscripts and subscripts			
b	baseline	m	monitoring
Abbreviations			
CON	Condenser	CP	Condensate pump
DEA	Deaerator	ECO	Economizer
EG	Electric generator	HPT	High pressure turbine
IPT	Intermediate pressure turbine	LPT	Low pressure turbine
LTRH	Low temperature reheater	LTSH	Low temperature reheater
RH	Reheater	SH	Superheater
SR	Shunt regulator	SSH	Screen-type superheater
WHRS	Waste heat recovery system	WGS	Water gas shift

References

1. Vujanović, M.; Wang, Q.; Mohsen, M.; Duić, N.; Yan, J. Recent progress in sustainable energy-efficient technologies and environmental impacts on energy systems. *Appl. Energy* **2020**, *283*, 116280. [CrossRef]
2. Zhao, Y.; Liu, M.; Wang, C.; Wang, Z.; Chong, D.; Yan, J. Exergy analysis of the regulating measures of operational flexibility in supercritical coal-fired power plants during transient processes. *Appl. Energy* **2019**, *253*, 113487. [CrossRef]
3. Cao, R.; Lu, Y.; Yu, D.; Guo, Y.; Bao, W.; Zhang, Z.; Yang, C. A novel approach to improving load flexibility of coal-fired power plant by integrating high temperature thermal energy storage through additional thermodynamic cycle. *Appl. Therm. Eng.* **2020**, *173*, 115225. [CrossRef]
4. Szima, S.; del Pozo, C.A.; Cloete, S.; Chiesa, P.; Alvaro, J.; Cormos, A.-M.; Amini, S. Finding synergy between renewables and coal: Flexible power and hydrogen production from advanced IGCC plants with integrated CO_2 capture. *Energy Convers. Manag.* **2021**, *231*, 113866. [CrossRef]
5. Wang, B.; Ma, H.; Ren, S.; Si, F. Effects of integration mode of the molten salt heat storage system and its hot storage temperature on the flexibility of a subcritical coal-fired power plant. *J. Energy Storage* **2023**, *58*, 106410. [CrossRef]
6. Wang, C.; Song, J. Performance assessment of the novel coal-fired combined heat and power plant integrating with flexibility renovations. *Energy* **2023**, *263*, 125886. [CrossRef]
7. Ouyang, T.; Qin, P.; Tan, X.; Wang, J.; Fan, J. A novel peak shaving framework for coal-fired power plant in isolated microgrids: Combined flexible energy storage and waste heat recovery. *J. Clean. Prod.* **2022**, *374*, 133936. [CrossRef]
8. Acaroğlu, H.K.H.M. Testing the environmental Kuznets curve hypothesis in terms of ecological footprint and CO_2 emissions through energy diversification for Turkey. *Environ. Sci. Pollut. Res.* **2023**. [CrossRef]
9. Harrucksteiner, A.; Thakur, J.; Franke, K.; Sensfuß, F. A geospatial assessment of the techno-economic wind and solar potential of Mongolia. *Sustain. Energy Technol. Assess.* **2023**, *55*, 102889. [CrossRef]
10. Bhanja, R.; Roychowdhury, K. A spatial analysis of techno-economic feasibility of solar cities of India using Electricity System Sustainability Index. *Appl. Geogr.* **2023**, *154*, 102893. [CrossRef]
11. Wang, C.; Raza, S.A.; Adebayo, T.S.; Yi, S.; Shah, M.I. The roles of hydro, nuclear and biomass energy towards carbon neutrality target in China: A policy-based analysis. *Energy* **2023**, *262*, 125303. [CrossRef]
12. Timilsina, G.R. The economics of deploying distributed solar photovoltaics in developing countries: Some insights from an analysis for Bangladesh. *Energy Sustain. Dev.* **2022**, *70*, 247–258. [CrossRef]
13. Wang, D.; Liu, D.; Wang, C.; Zhou, Y.; Li, X.; Yang, M. Flexibility improvement method of coal-fired thermal power plant based on the multi-scale utilization of steam turbine energy storage. *Energy* **2022**, *239*, 122301. [CrossRef]
14. Gu, Y.; Xu, J.; Chen, D.; Wang, Z.; Li, Q. Overall review of peak shaving for coal-fired power units in China. *Renew. Sustain. Energy Rev.* **2016**, *54*, 723–731. [CrossRef]
15. Meng, Y.; Cao, Y.; Li, J.; Liu, C.; Li, J.; Wang, Q.; Cai, G.; Zhao, Q.; Liu, Y.; Meng, X.; et al. The real cost of deep peak shaving for renewable energy accommodation in coal-fired power plants: Calculation framework and case study in China. *J. Clean. Prod.* **2022**, *367*, 132913. [CrossRef]

16. Starkloff, R.; Alobaid, F.; Karner, K.; Epple, B.; Schmitz, M.; Boehm, F. Development and validation of a dynamic simulation model for a large coal-fired power plant. *Appl. Therm. Eng.* **2015**, *91*, 496–506. [CrossRef]
17. Uruno, Y.; Choi, G.; Sung, M.; Chung, J.; Kim, H.; Lee, K. Transient analysis of attemperator enthalpy balance based on the commissioning data of a coal-fired steam power plant. *Appl. Therm. Eng.* **2019**, *150*, 1141–1158. [CrossRef]
18. Zhao, Y.; Fan, P.; Wang, C.; Liu, M.; Chong, D.; Yan, J. Fatigue lifetime assessment on a high-pressure heater in supercritical coal-fired power plants during transient processes of operational flexibility regulation. *Appl. Therm. Eng.* **2019**, *156*, 196–208. [CrossRef]
19. Yuan, Y.; Bai, Z.; Liu, Q.; Hu, W.; Zheng, B. Potential of applying the thermochemical recuperation in combined cooling, heating and power generation: Route of enhancing the operation flexibility. *Appl. Energy* **2021**, *301*, 117470. [CrossRef]
20. Yan, H.; Liu, M.; Wang, Z.; Zhang, K.; Chong, D.; Yan, J. Flexibility enhancement of solar-aided coal-fired power plant under different direct normal irradiance conditions. *Energy* **2023**, *262*, 125349. [CrossRef]
21. Xue, Y.; Ge, Z.; Yang, L.; Du, X. Peak shaving performance of coal-fired power generating unit integrated with multi-effect distillation seawater desalination. *Appl. Energy* **2019**, *250*, 175–184. [CrossRef]
22. Hentschel, J.; Zindler, H.; Spliethoff, H. Modelling and transient simulation of a supercritical coal-fired power plant: Dynamic response to extended secondary control power output. *Energy* **2017**, *137*, 927–940. [CrossRef]
23. Wang, C.; Zhao, Y.; Liu, M.; Qiao, Y.; Chong, D.; Yan, J. Peak shaving operational optimization of supercritical coal-fired power plants by revising control strategy for water-fuel ratio. *Appl. Energy* **2018**, *216*, 212–223. [CrossRef]
24. Zhao, Y.; Liu, M.; Wang, C.; Li, X.; Chong, D.; Yan, J. Increasing operational flexibility of supercritical coal-fired power plants by regulating thermal system configuration during transient processes. *Appl. Energy* **2018**, *228*, 2375–2386. [CrossRef]
25. Wang, C.; Liu, Z.; Fan, M.; Zhao, Y.; Liu, M.; Yan, J. Enhancing the flexibility and efficiency of a double-reheat coal-fired power unit by optimizing the steam temperature control: From simulation to application. *Appl. Therm. Eng.* **2022**, *217*, 119240. [CrossRef]
26. Ma, J.; Zamarripa, M.A.; Eslick, J.C.; Le, Q.M.; Bhattacharyya, D.; Biegler, L.T.; Zitney, S.E.; Burgard, A.P.; Miller, D.C. Computer Aided Chemical Engineering. In *Dynamic Simulation and Optimization of a Subcritical Coal-Fired Power Plant During Load-Ramping Operations*; Yamashita, Y., Kano, M., Eds.; Elsevier: Amsterdam, The Netherlands, 2022; pp. 1033–1038.
27. Yan, H.; Liu, M.; Chong, D.; Wang, C.; Yan, J. Dynamic performance and control strategy comparison of a solar-aided coal-fired power plant based on energy and exergy analyses. *Energy* **2021**, *236*, 121515. [CrossRef]
28. Dai, B.; Wang, F.; Chang, Y. Multi-objective economic load dispatch method based on data mining technology for large coal-fired power plants. *Control Eng. Pract.* **2022**, *121*, 105018. [CrossRef]
29. Ma, T.; Li, M.-J.; Xu, J.-L.; Ni, J.-W.; Tao, W.-Q.; Wang, L. Study of dynamic response characteristics of S-CO_2 cycle in coal-fired power plants based on real-time micro-grid load and a novel synergistic control method with variable working conditions. *Energy Convers. Manag.* **2022**, *254*, 115264. [CrossRef]
30. Wang, C.; Liu, M.; Li, B.; Liu, Y.; Yan, J. Thermodynamic analysis on the transient cycling of coal-fired power plants: Simulation study of a 660 MW supercritical unit. *Energy* **2017**, *122*, 505–527. [CrossRef]
31. Dynasim AB; Dassault Systèmes. *Dymola User Manual*; Dassault Systèmes AB: Lund, Sweden, 2021.
32. Wang, K. *Research on the Performance Evaluation Method of Load Control Systems Combining "Two Rules"*; North China Electric Power University: Beijing, China, 2021.
33. Yinsong, W.; Shizhe, L.; Jingyu, T.; Zheng, Z. Performance assessment of thermal power plant load control system based on covariance index. *Control Eng. Pract.* **2016**, *54*, 58–69. [CrossRef]
34. Yu, J.; Qin, S.J. Statistical MIMO controller performance monitoring. Part I: Data-driven covariance benchmark. *J. Process Control* **2008**, *18*, 277–296. [CrossRef]
35. Yu, J.; Qin, S.J. Statistical MIMO controller performance monitoring. Part II: Performance diagnosis. *J. Process Control* **2008**, *18*, 297–319. [CrossRef]